ELSEVIER

Nuclear Instruments and Methods in Physics Research A 480 (2002) 456–462

NUCLEAR INSTRUMENTS & METHODS IN PHYSICS RESEARCH Section A

www.elsevier.com/locate/nima

Measurement of the dispersion law for hydrophobic silica aerogel SP-25

M.F. Villoro[a], J.C. Plascencia[a], R. Núñez[a], A. Menchaca-Rocha[b,*], J.M. Hernández[b], E. Camarillo[b], M. Buénerd[c]

[a] *Facultad de Ciencias, UNAM, Ciudad Universitaria, 04510 Mexico D.F., Mexico*
[b] *Instituto de Fisica, UNAM, A.P. 20-364, 01000 Mexico D.F., Mexico*
[c] *Institut des Sciences Nucléaires, IN2P3-CNRS and Université Joseph Fourier, 53 Ave. des Martyrs, F-38026 Grenoble Cédex, France*

Received 15 November 2000; received in revised form 6 March 2001; accepted 24 March 2001

Abstract

Optical properties of hydrophobic silica aerogel SP-25 have been measured. These include: a seven point dispersion law $n(\lambda = 266.2 - 514.5\ \text{nm})$, absorbance, luminescence and other physical properties. The effect of chromatic dispersion on velocity resolution for an aerogel-based RICH counter was estimated. © 2002 Elsevier Science B.V. All rights reserved.

PACS: 78.20.Ci; 29.40.Ka; 98.70.Sa

Keywords: Cherenkov counters; Cosmic-ray detection; Cherenkov radiators; Aerogel; Refractive index; Chromatic dispersion

1. Introduction

Silica aerogels (AGL) have been produced with a broad range of refraction indices, from 1.006 to 1.14 [1,2], bridging the gap between gas and solid (liquid) Cherenkov radiators. This explains their wide use in Cherenkov instrumentation, both as threshold and imaging [3] counters. In spite of it, only the optical properties of some versions of these materials have been investigated [4], while the rest are scarcely documented. Concerning Cosmic Ray applications, AGL counters have been operated on balloon and satellite experiments [5]. Caprice was the first balloon experiment to use a (gas) Ring Imaging Cherenkov (RICH) counter [6], and the Alpha Magnetic Spectrometer (AMS) will be the first experiment to implement an AGL-based RICH counter on a satellite experiment [7].

The resolution of a RICH counter is physically limited by the optical dispersion of its radiator. A good knowledge of the latter is thus necessary for the design of this type of counter. Due to a lack of experimental data, the AGL dispersion law is usually evaluated using the scaling rule based on the Lorentz–Lorenz law [8,9]. Although this procedure is expected to give good results, it is clearly calling for an experimental confirmation.

The prospective use of hydrophobic silica aerogel radiators in the AMS Project [9] makes it

*Corresponding author. Tel.: +52-525-6225060; fax: +52-525-6161535.

E-mail addresses: amen@servidor.unam.mx (A. Menchaca-Rocha).

0168-9002/02/$ - see front matter © 2002 Elsevier Science B.V. All rights reserved.
PII: S0168-9002(01)00956-1

important to carry out a thorough physical characterization of this material. Previous research was carried out [10] for an SP-30 version of it, used for the threshold counter which was flown aboard the Space Shuttle "Discovery" in the STS-91 mission in 1998. The Physics program of the forthcoming phase of the AMS experiment has prompted the development of a less dense ($\rho = 0.09$ g/cm^3), SP-25 AGL[1] having nominal refractive index $n = 1.025$, for the RICH counter. Here we report on an investigation designed to measure the relevant optical properties necessary to estimate the uncertainty in velocity determinations associated with chromatic dispersion, as part of an effort to establish the suitability of this material for use in the second AMS mission on the International Space Station (ISS), scheduled for the end of year 2003.

The measurements reported here are: (a) absorbance, (b) luminescence induced by UV ($\lambda = 220$ nm) light, (c) electron-microscope determination of the mean nanostructure radii, and (d) refractive index determination at $\lambda = 266.2, 354.9, 476.5, 488.0, 496.5, 501.7,$ and 514.5 nm. The latter allowed us to determine an approximate dispersion law, based on the Sellmeier [11] empirical formula. Combined with the quantum efficiency of the photomultiplier (PMT) tubes which are being considered for this application, this information is then used to estimate the expected uncertainty in velocity determinations introduced by chromatic dispersion in the AMS–RICH.

2. Experiment

2.1. Absorbance, luminescence, and nanostructure measurements

Room temperature optical absorption spectra were obtained with a Milton Roy Spectrophotometer Model 3000 in the 220–900 nm range. The resulting absorbance spectrum is shown in Fig. 1, where a broad absorption band is observed in the UV region.

[1] Matsushita Electric Works, Ttd., Osaka, Japan.

A Perkin Elmer Model 610S Spectrofluorimeter was used to measure the photoluminescence spectrum shown in Fig. 2. The incident $\lambda_i = 220$ nm light was chosen to fall within the absorbance band shown in Fig. 1. Here we observe a broad structure centered around 400 nm. The structures in the vicinity of 440 nm correspond to 1st harmonic (i.e., $\lambda \times 2$) contamination.

A $250,000\times$ amplified image of an SP-25 aerogel sample was also taken (not shown) using a transmission electron microscope JEOL 100CX set to 100 keV. This allowed us to determine that the average aerogel nanostructure size is 15 ± 5 nm.

2.2. Dispersion law

Refractive indices were measured using the experimental arrangement shown schematically in Fig. 3 using single $\lambda = 476.5, 488.0, 496.5, 501.7,$ 514.5 nm lines of a continuous wave 3W Argon Ion of Spectra Physics Model 2020 and harmonic $\lambda = 266.2, 354.9$ nm lines of an Nd:YAG pulsed laser (10 ns wide). As a detection unit we used a photodiode masked with a narrow (0.1 mm) vertical slit, and mounted on a 0.05 mm precision scale, to scan across light spots observed along the line P, located at a distance l from the sample. Measuring the position of maximum light intensity of both the unrefracted and refracted beams, allowed us to determine the distance $d(\theta)$. Using $\delta = \arctan(d/l)$, and Snell's law, the following equation applies for the experimental setup of Fig. 3:

$$\delta = \eta + \theta - \alpha + \sin^{-1}\left(n \sin\left(\alpha - \sin^{-1}\left(\frac{\sin(\eta + \theta)}{n}\right)\right)\right). \tag{1}$$

In our case $\alpha = 90^\circ$ (i.e., square sample), $l = 1999.5$ mm ± 1 mm, and η is a parameter reflecting our uncertainty concerning the $\theta = 0^\circ$ position. As is known, for a given value of n, δ has a well defined minimum as a function of θ. This fact is commonly used [10,12] to extract values of n, by simply searching for the corresponding minimum value of d. This method has the

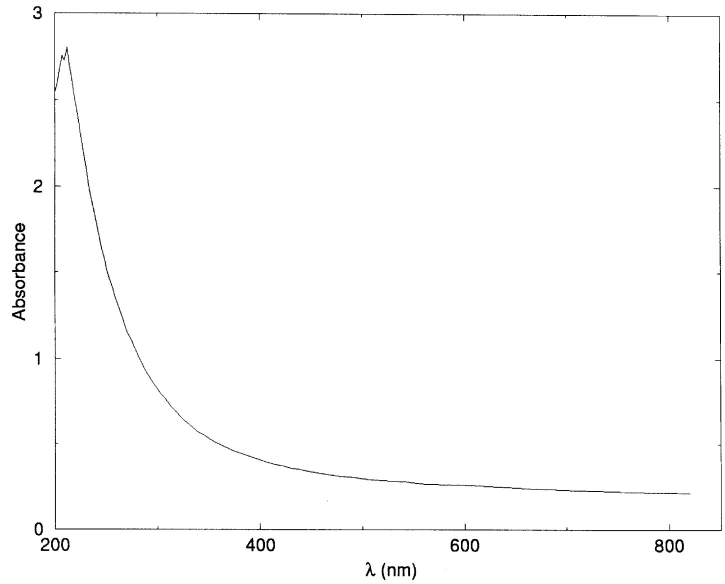

Fig. 1. Absorbance spectrum for a 1.0 cm thick sample of SP-25 silica AGL. Data below $\lambda = 220$ nm are affected by instrumental limitations.

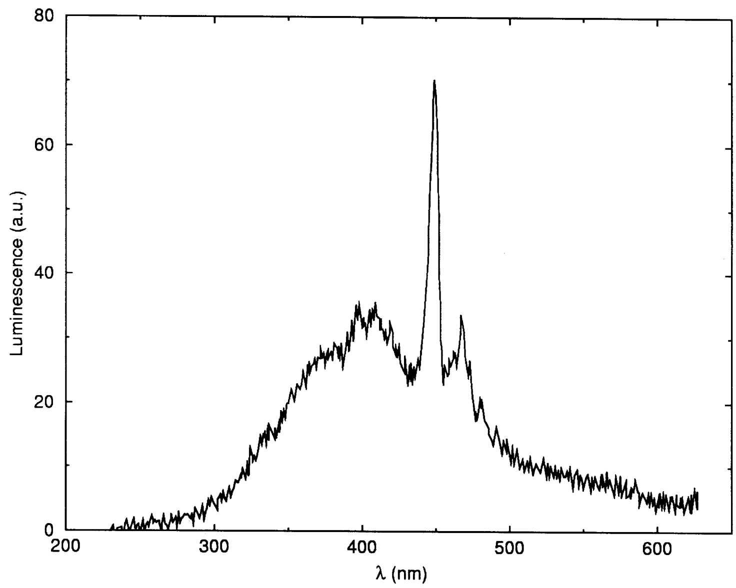

Fig. 2. Luminescence spectrum of SP-25 silica AGL excited by $\lambda_i = 220$ nm light.

advantage of avoiding a precise determination of θ, relying only on how well the minimum d value can be established. Here we use an alternative method, in which several measurements of d, around the expected minimum (using Eq. (1)) are performed by rotating the sample, thereby varying the angle θ. This technique has the apparent disadvantage of introducing a new parameter (η).

Yet, a number of d measurements larger than 2 lead to an overdetermination which can be used to reduce the uncertainty in the refractive index. This was achieved through a minimum χ^2 fitting of the $\delta(\theta)$ data using Eq. (1), leaving n and η as free parameters. The resulting n values and their corresponding uncertainties are listed in Table 1, and plotted as function of λ in Fig. 4. The continuous line joining the points represents the Sellmeier fit described in the next section. Note that the AGL manufacturer[1] provides an empirical $n = 1.0 + 0.277\rho$ relationship which, when used with the n values found at large wavelengths (≈ 1.027) indicates that the density of our sample is higher (≈ 0.097 g/cm^3) than the nominal value.

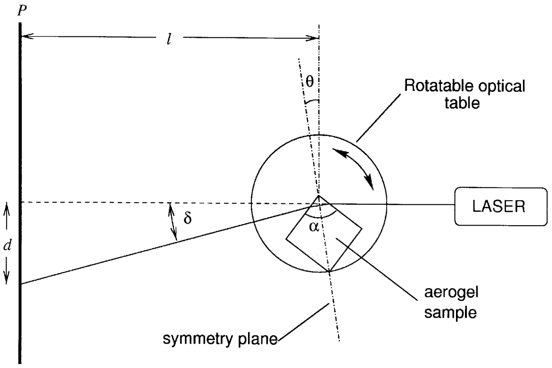

Fig. 3. Schematic experimental setup.

3. Discussion

The single-pole Sellmeier function:

$$n^2 = 1 + \frac{a_0\lambda^2}{\lambda^2 - \lambda_0^2} \tag{2}$$

Table 1
Measured refractive indices (n) and uncertainties

λ (nm)	n	$\pm$	Percentage of error in ($n-1$) (%)
266.2	1.03001	0.00041	1.37
354.9	1.02820	0.00041	1.45
476.5	1.02756	0.00044	1.59
488.0	1.02726	0.00061	2.24
496.5	1.02730	0.00054	1.98
501.7	1.02729	0.00046	1.68
514.5	1.02744	0.00041	1.49

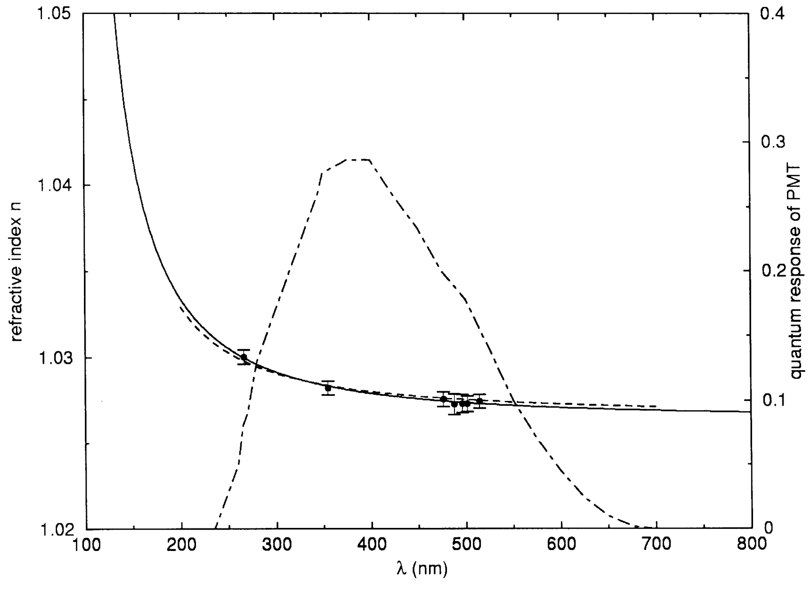

Fig. 4. SP-25 Dispersion Law, measurements and single-pole Sellmeier fit. The dot-dashed curve represents the PMT quantum efficiency, and the dashed line is the scaling law prediction.

has been used to fit the data from Table 1, using the minimum χ^2 criterion while leaving a_0 and λ_0 as free parameters. The resulting curve is represented as a solid line in Fig. 4, corresponding to the values of $a_0 = 0.05359 \pm 0.00032$ and $\lambda_0 = 91.82 \pm 3.82$ nm.

From Eq. (2) and from the errors of the Sellmeier parameters, an estimate of the error of n is obtained in the usual way for any wavelength in the range of highest PMT quantum response (dot-dashed curve in Fig. 4), as shown in Fig. 5. The relative error in $(n-1)$ does not exceed 1.5% within the PMT quantum efficiency window. The number N of photons emitted, per unit wavelength, and per unit length traversed by a $Z = 1$ particle of a Cherenkov-emitting material, is given by

$$\frac{\mathrm{d}N}{\mathrm{d}\lambda\,\mathrm{d}x} = 2\pi\alpha\frac{1}{\lambda^2}\left(1 - \frac{1}{\beta^2 n^2}\right)\mathrm{e}^{-\mu d(x)} \tag{3}$$

where α is the fine structure constant, β is the particle velocity (relative to c, light's speed), and μ is the absorption coefficient calculated from the absorbance measurements (Fig. 1), and $d(x)$ is the thickness of AGL traversed by a photon emitted at point x [13]. For a particle incident perpendicularly to the AGL, $d(x) = x/\cos\theta_C$, where θ_C is the Cherenkov angle, so that $d(x) = x\beta n$. Eq. (3) has been integrated over x to estimate the number of photons detected by an ideal RICH detector having a 1 cm thick radiator, as a function of refractive index (Fig. 6), for three particle velocities. The very small photon losses due to internal reflection, estimated using Fresnel's equations, have also been included in this calculation.

The information in Fig. 6 allowed us to estimate a mean refractive index of $\langle n \rangle = 1.02815$ with a standard deviation $\Delta n = 0.00078$. Hence, the use of SP-25 AGL as radiator corresponds to Cherenkov emission threshold of ≈ 3.1 GeV/A kinetic energy. The ratio

$$\frac{\Delta n}{\langle n \rangle} = 0.076\% \tag{4}$$

provides a good estimate of the uncertainty in n introduced by the chromatic dispersion of a unit-length (1.0 cm) radiator, taking into account the quantum efficiency of the PMTs. The information in Fig. 2 was used to estimate the combined effect on $\Delta n/\langle n \rangle$ of absorptive phenomena, mainly

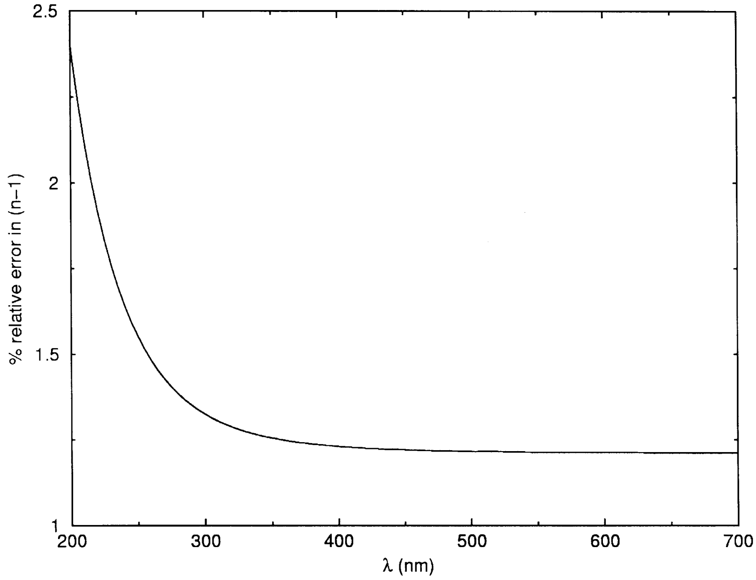

Fig. 5. Refractive index worst-case uncertainty as a function of λ.

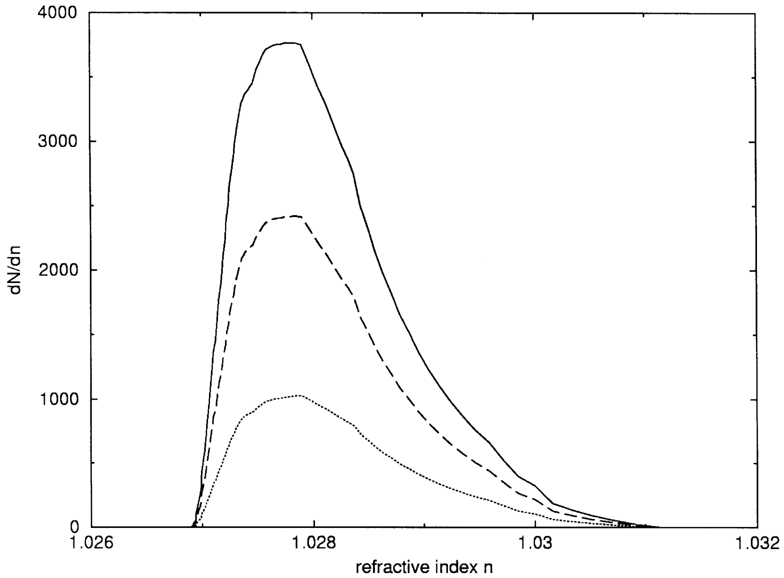

Fig. 6. Number of photons detected vs refractive index for $\beta = 0.98$ (dotted), 0.99 (dashed), and 1.0 (continuous).

fluorescence and Rayleigh dispersion, which turned out to be negligible ($\leqslant 0.001\%$).

Since, on the first approximation,

$$\frac{\Delta n}{\langle n \rangle} \approx \frac{\Delta \beta}{\beta} \quad (5)$$

the limitations on velocity resolution associated with the use of 1.0 cm-thick SP-25 hydrophobic aerogel radiators in the AMS–RICH, should lie within the 0.1% range. It is interesting to note that the use of 1 cm thick AGL radiators with a ≈ 40 cm drift gap introduces geometrical uncertainties on $\Delta\beta/\beta$ which are of the same 0.1% order of magnitude.

Finally, Fig. 4 also compares our dispersion law measurements with scaling rule predictions (dashed line), derived from the Lorentz–Lorenz law [8], using the known n values for fused silica [14]. The remarkable agreement confirms the relevancy of the scaling rule applied in Ref. [9].

4. Conclusion

The dispersion law of AGL SP-25 has been measured within the region of sensitivity of the AMS–RICH PMTs. Our measurements show that the refractive index variation in this domain lies within the 0.1% range, indicating that the uncertainties introduced by the use of a unit length of this material has an equivalently small effect on velocity determinations. The use of scaling to estimate the dispersion law for low density AGL from fused silica data is also validated by our data.

Acknowledgements

We are indebted to Prof. S.C.C. Ting for his support and encouragement, to the Matsushita Company (M. Yokoyama) for generously providing the SP-25 samples, and to M. Rangel, R. Hernández, and L. Martínez for their technical assistance. We also acknowledge the partial support of CNRS-CONACYT (project E130-493) and DGAPA-UNAM (project IN101599).

References

[1] G. Poelz, R. Riethmüller, Nucl. Instr. and Meth. A 195 (1982) 491. I. Adachi, et al., Nucl. Instr. and Meth. A 355 (1995) 390.

[2] H. Yokogawa, M. Yokoyama, J. Non-Cryst. Solids 186 (1995) 23.

[3] D.E. Fields, et al., Nucl. Instr. and Meth. A 349 (1994) 431. R. De Leo, et al., Nucl. Instr. and Meth. A 401 (1997) 187. E. Nappi, Nucl. Phys. B B61 (1998) 270.
[4] E. Aschenauer, et al., Nucl. Instr. and Meth. A 440 (2000) 338. R. De Leo, et al., Nucl. Instr. and Meth. A 457 (2001) 52.
[5] M. Cantin, et al., Nucl. Instr. and Meth. 118 (1974) 177. Y. Asaoka, et al., Nucl. Instr. and Meth. A 416 (1998) 236.
[6] P. Carlson, et al., Nucl. Instr. and Meth. A 349 (1994) 577.
[7] S.C.C. Ting, Phys. Rep. 279 (1997) 203.
[8] M. Born, A. Wolf, Principle of Optics, Pergamon, 1975. M. Buénerd, AMS Internal Note AMS/2000_05_05.
[9] M. Buénerd, Z. Ren, Nucl. Instr. and Meth. A 454 (2000) 478.
[10] A.K. Gougas, D. Ilie, S. Ilie, V. Pojidaev, Nucl. Instr. and Meth. A 421 (1999) 249.
[11] J. Morgan, Introduction to Geometrical and Physical Optics, McGraw-Hill, New York.
[12] P. Wang, A. Beck, W. Körner, H. Scheller, J. Fricke, J. Phys. D 27 (1994) 414.
[13] J.D. Jackson, Classical Electrodynamics, 2nd Edition, Wiley, New York, 1975.
[14] W.G. Driscoll, W. Vanghan (Eds.), Handbook of Optics, McGraw Hill, New-York, 1995.